XLI CILAMCE
XLI Ibero-Latin American Congress on Computational Methods in Engineering
16-19 November, 2020 FOZ DO IGUAÇU PARANÁ - BRAZIL

Direct numerical simulation of a sphere settling in a thixo-viscoplastic fluid using lattice Boltzmann method

Marco A. Ferrari[1], Alan Lugarini[1], Admilson T. Franco[1]

[1]*Research Center for Rheology and Non-Newtonian Fluids (CERNN), Universidade Tecnológica Federal do Paraná (UTFPR)*
Deputado Heitor Alencar Furtado Street, 5000, 81290-000, Curitiba - PR, Brazil
marcoferrari@alunos.utfpr.edu.br, alansouza@utfpr.edu.br, admilson@utfpr.edu.br

Abstract. During a drilling operation of oil and gas wellbores it is sometimes necessary to stop fluid pumping, and this causes the cuttings to settle towards the bottom. To avoid cuttings from accumulating downhole, drilling fluids are designed for gelification, which in rheologic terms means the build-up of yield stress in a thixotropic material. To study this phenomenon, the lattice Boltzmann method (LBM) is utilized to solve fluid flow while the immersed boundary method (IBM) is employed to solve the motion of a spherical particle. Thixotropy is modeled with a structural parameter model, whose scalar is associated with the fluid's yield stress. The structural parameter is transported by the convection-diffusion equation in the mesoscopic scale. The focus of the present work is on the effects of model parameters on the trajectory and terminal velocity of a spherical particle released from the rest in a thixotropic fluid initially fully unstructured. Considering that the fluid starts to age as soon as the sphere is released, the particle velocity decreases because of the increased yield stress and after a while reaches its terminal velocity. If the maximum yield stress is increased above a threshold, the particle is not capable to break through the new structured fluid and ceases to move after some time, staying suspended in the gelified fluid.

Keywords: Particle Settling, Thixotropy, Lattice Boltzmann Method, Immersed boundary Method.

1 Introduction

The interaction between a fluid medium and a settling particle is a critical process for some industries, such as in drilling of oil and gas wellbores where the removed cuttings are transported to the surface by the drilling fluids. These fluids often exhibit thixotropy, a time-dependent property on which the fluid has a reduction in the viscosity due to the action of shear during a period[1]. This allows the fluid to be easily pumped when the at steady-state and reduce the terminal velocity of the cuttings in the case of stop circulation. Another important property that drilling fluids may present is the viscoplasticity. Viscoplastic fluids have yield stress, which corresponds to the minimal stress for the fluid start to flow [2]. This also applies to the settling phenomenon: if the particle does not have enough weight to surpass the yield stress, it will remain static in the fluid [3]. This is important because the drilling fluid is correctly formulated it will retain a part of the cuttings, which otherwise would accumulate in the bottom of the borehole and that could lead to stuck the pipe.

Some studies analyzed the settling phenomenon of one or two particles in thixotropic fluids [4, 5], using Laponite and Xanthan gum solutions respectively. For the Laponite solution it was observed the longer the fluid remained untouched, the lower the particle velocity, until a certain point where would be retained by the fluid. Meanwhile for Xanthan gum experiment, a leading particle created a path of reduced viscosity, which made a trailing particle have increased settling velocity.

To further understand the events that occur during the particle settling in a thixo-viscoplastic fluid, a direct numerical simulation (DNS) based on the lattice Boltzmann method (LBM) will be used. The LBM is coupled with the immersed boundary method (IBM) to model the particle motion. A detached boundary composed of Lagrangian nodes applies a force in the fluid, modeling a wall in that location. Thixotropy may be modeled in several ways [6]. One of them is the indirect microstructural model, which uses a scalar denominated structural parameter to define the structuring level of the fluid. This allows the fluid properties, such as yield stress and plastic viscosity, to be associated with the numerical value of the structural parameter. Being an intensive property, the convection-diffusion transport equation in the mesoscopic scale is utilized to calculate its value in the flow. It will

be analyzed the particle behavior, trajectory and velocity, as function of the yield number and model parameters as well as the condition for the particle be retained by the fluid.

2 Numerical Method

The lattice Boltzmann method (LBM) is based on the discretization of the Boltzmann equation in the mesoscopic scale. The method solves the behavior of a group of particles that travel in the discrete phase space. One of the points in the discrete form of the Boltzmann equation is how to discretize the collision operator. An option is to utilize the BGK collision operator proposed by Bhatnagar et al. [7]. This method utilizes a single relaxation time, which for some cases exhibits numerical instabilities. Later developments improved the stability, one of them is the method proposed by Latt and Chopard [8] which uses regularized pre-collision particle populations. By this method the discrete Boltzmann equation is:

$$f_i\left(\boldsymbol{x}+c_i\Delta t, t+\Delta t\right)=\left(1-\frac{1}{\tau}\right)f_i^{reg}\left(\boldsymbol{x},t\right)+\frac{1}{\tau}f_i^{eq}\left(\boldsymbol{x},t\right)+\left(1-\frac{1}{2\tau}\right)F_i\left(\boldsymbol{x},t\right)\Delta t, \tag{1}$$

where f_i is the particle distribution function in a point $\boldsymbol{x}$ in the time t, F_i is the body force acting in that point, τ is the relaxation time, f^{eq} is the particle equilibrium distribution function, which in the discrete form is [9]:

$$f_i^{eq}=w_i\rho\left[1+\frac{c_{i\alpha}u_\alpha}{c_s^2}+\frac{u_\alpha u_\beta\left(c_{i\alpha}c_{i\beta}-c_s^2\delta_{\alpha\beta}\right)}{2c_s^4}\right], \tag{2}$$

where ρ is the fluid density, w_i is the velocity direction weight, u_α is the fluid velocity in the α Cartesian coordinate direction, c_s is the speed of the sound, and $c_{i\alpha}$ is the velocity vector which depends in the velocity set utilized. For the D3Q7 and D3Q19 velocity sets, the values for c_i and w_i are, respectively:

$$c_i=\begin{cases}(0,0,0), & i=0 & w_i=1/4\\ (\pm1,0,0),(0,\pm1,0),(0,0,\pm1), & i=1,...,6 & w_i=1/8\end{cases} \tag{3a}$$

$$c_i=\begin{cases}(0,0,0), & i=0 & w_i=1/3\\ (\pm1,0,0),(0,\pm1,0),(0,0,\pm1), & i=1,...,6 & w_i=1/18\\ (\pm1,\pm1,0),(\pm1,0,\pm1),(0,\pm1,\pm1), & i=7,...,19 & w_i=1/36\end{cases} \tag{3b}$$

The transformation of the body force term present in the eq. (1) from the Cartesian system to a velocity set is [10]:

$$F_i=w_i\left[\frac{c_{i\alpha}}{c_s^2}+\frac{\left(c_{i\alpha}c_{i\beta}-c_s^2\delta_{\alpha\beta}\right)u_\beta}{c_s^4}\right]F_\alpha \tag{4}$$

The current equations deal with the behavior of particle populations over time and space. For engineering problems it is necessary to know the macroscopic properties of the flow. Density, velocity and the viscous stress tensor can be computed as [11]:

$$\rho=\sum_i f_i+\frac{\Delta t}{2}\sum_i F_i \tag{5}$$

$$\rho u_\alpha=\sum_i f_i c_{i\alpha}+\frac{\Delta t}{2}\sum_i F_i c_{i\alpha} \tag{6}$$

$$\sigma_{\alpha\beta}\approx\Pi_{\alpha\beta}^{neq}=-\left(1-\frac{\Delta t}{2\tau}\right)\sum_i\left(f_i-f_i^{eq}\right)c_{i\alpha}c_{i\beta}-\frac{\Delta t}{2}\left(1-\frac{\Delta t}{2\tau}\right)\left(F_\alpha u_\beta+u_\alpha F_\beta\right) \tag{7}$$

To return the momentum balance equations it is necessary a relation of the properties and momentum balance of generalized Newtonian fluids between the mesoscopic and macroscopic scales. This is accomplished by correlation of the apparent viscosity and the relaxation time, which originates from the Chapman–Enskog expansion [12]:

$$\tau = \frac{\eta}{\rho c_s^2} + \frac{\Delta t}{2}. \tag{8}$$

As effect, changing the relaxation time locally the fluid viscosity will also change. The thixotropic model utilized in this work is a reduced model adapted from the indirect microstructural model proposed by Houska [13]:

$$\sigma = \eta(\dot{\gamma}, \lambda)\dot{\boldsymbol{\gamma}}, \tag{9a}$$

$$\eta(\dot{\gamma}, \lambda) = \begin{cases} \infty & ,|\sigma| \leq \tau_y \\ \eta_p + \tau_y/|\dot{\gamma}| & ,|\sigma| > \tau_y \end{cases} \tag{9b}$$

$$\tau_y = \lambda \tau_y^S + (1-\lambda)\,\tau_y^D \tag{9c}$$

$$\frac{\partial \lambda}{\partial t} + u_i \frac{\partial \lambda}{\partial x_i} = \frac{1}{t_{eq}}\left[-k_1 \lambda \dot{\gamma} + k_2(1-\lambda)\right], \tag{9d}$$

where λ is the structural parameter responsible for the thixotropy, τ_y^S is the static yield stress, τ_y^D is the dynamic yield stress, η_p is the plastic viscosity, $\dot{\gamma}$ is the shear rate, t_{eq} is the equilibrium time, k_1 and k_2 are the breakdown and build-up parameters respectively. To transport the structural parameter over the flow, the convection-diffusion equation in the mesoscopic scale is utilized [14]:

$$g_i\left(\boldsymbol{x} + c_i \Delta t, t + \Delta t\right) = \left(1 - \frac{1}{\tau_g}\right) g_i\left(\boldsymbol{x}, t\right) + \frac{1}{\tau_g} g_i^{eq}\left(\boldsymbol{x}, t\right) + \left(1 - \frac{1}{2\tau_g}\right) w_i q\left(\boldsymbol{x}, t\right), \tag{10}$$

$$g_i^{eq} = w_i \lambda \left[1 + \frac{c_{i\alpha} u_\alpha}{c_s^2} + \frac{u_\alpha u_\beta \left(c_{i\alpha} c_{i\beta} - c_s^2 \delta_{\alpha\beta}\right)}{2 c_s^4}\right] \tag{11}$$

$$\tau_g = \frac{\mathfrak{D}}{c_s^2} + \frac{\Delta t}{2} \tag{12}$$

$$\lambda = \sum_i g_i + \left(1 - \frac{1}{2\tau_g}\right) \frac{w_i \Delta t}{2} q \tag{13}$$

where g_i is the particle distribution function associated with the structural parameter λ, τ_g is the relaxation time associated with diffusion factor of the structural parameter $\mathfrak{D}$ (necessary to be close to 0.5 to avoid numeric diffusion), and q is the source term responsible for the breakdown and build-up of the fluid-structure and it is equal to the right hand side of the eq. (9d). This second population group (g_i) will utilize the velocity set D3Q7 [15] while the population responsible for the fluid flow (f_i) utilizes the D3Q19.

To model a particle settling in the thixotropic fluid the immersed boundary method (IBM)[16][17] is utilized. This method consists in a second mesh composed of Lagrangian nodes that apply a body force in the fluid discretized by the Eulerian lattices. Because the nodes do not necessarily coincide with lattices, the force exerted by the node is distributed over a region by a discrete Dirac's delta[16], in this work is determined by the kernel ϕ_4. The no-slip condition is then satisfied when the velocity of the IBM nodes is equal to the interpolation of the fluid velocity from the LBM:

$$\boldsymbol{u}^L = \sum_E \boldsymbol{u}^{E,noF} \delta\left(\boldsymbol{x} - \boldsymbol{X}\right) h^3 + \sum_E \left[\sum_L \frac{\Delta t}{2\rho} \boldsymbol{F}^L \delta\left(\boldsymbol{x} - \boldsymbol{X}\right) \Delta S\right] \delta\left(\boldsymbol{x} - \boldsymbol{X}\right) h^3 \tag{14}$$

where $\boldsymbol{u}^L$ is the velocity of the IBM node, and $\boldsymbol{u}^{E,noF}$ is the fluid velocity without the effect of the IBM force, δ is the discrete Dirac's delta, $\boldsymbol{x} - \boldsymbol{X}$ is the distance between the Lagrangian node and an Eulerian lattice, h is the lattice length, $\boldsymbol{F}^L$ is the force exerted by the IBM nodes, and ΔS is the surface area of the IBM node. To solve this linear equation system where $\boldsymbol{F}^L$ is the unknown variable in each time step, the explicit method by by Dash et al. [18] will be used.

The sum of all node forces is equal to the total force that the particle applies in the fluid, and vice-versa by Newton's third law of motion. Because IBM does not eliminate the fluid inside the boundary formed by the Lagrangian nodes, the correction proposed by Feng and Michaelides [19] is implemented. Gravitational and buoyancy forces are the two remaining forces acting in the particle. Finally, the discrete velocity update equation is

$$\boldsymbol{U}_p^{t+1} = \left(1 + \frac{\rho_f}{\rho_p}\right)\boldsymbol{U}_p^t - \frac{\rho_f}{\rho_p}\boldsymbol{U}_p^{t-1} + \frac{1}{m_p}\left[-\sum_{L_p}\boldsymbol{F}^L h\Delta S + (m_p - m_f)\,\boldsymbol{g}\right]\Delta t, \tag{15}$$

where $\boldsymbol{U}_p$ is the velocity of the center of mass of the particle, ρ_f/ρ_p is the density ratio between the fluid and particle, m_p is the particle mass, m_f is the fluid mass inside the particle, and $\boldsymbol{g}$ is the gravitational acceleration.

3 Validation

Since the chosen thixotropic model permits the existence of yielded and unyielded zones coexisting in the fluid, it is important to assess its capability to solve the yield surface and the viscous drag. The simplest model where this behavior exists would be in a non-thixotropic Bingham fluid. Because of that, the Stokes' drag coefficient, $C_s = F/3\pi\eta_p VD$, around a fixed sphere immersed in a Bingham fluid, where F is the force, is solved numerically to validate the numerical model. A sphere of diameter D is positioned inside a rectangular domain with dimensions 10D $\times$ 10D $\times$ 10D. The kinetic parameters, k_1 and k_2, are equal to 0 and the initial value for the structural parameter is 1. This makes the thixotropic fluid behave like a Bingham fluid. A uniform inlet velocity V is applied[20], resulting in a Reynolds number $\mathrm{Re}_D = DV/\eta_p = 1$. Meanwhile, the lateral boundaries of the domain have a free-slip condition[21]. The yield stress is modified to allow a range of Bingham numbers Bi = 2, 5, 10, 20, 40. The ratio of the distance between Lagrangian nodes and the Eulerian lattice size is approximately 1. The numerical results are compared with the correlation proposed by Blackery and Mitsoulis [22] using their numerical results and represented in Table 1.

Table 1. Sphere Stokes' drag coefficient in a Bingham fluid.

Bi	2	5	10	20	40
Present	6.41	11.9	20.2	35.9	65.7
Blackery and Mitsoulis [22]	5.55	10.9	18.9	33.8	61.1
$\lvert(\theta - \theta_{ref})/\theta_{ref}$	15.7%	9.68%	6.92%	6.33%	7.54%

The errors are in acceptable limit considering that sphere diameter was equivalent to 20 lattices. The numerical accuracy can be further improved by increasing the sphere diameter, which for this work was limited by the amount available memory in the GPU utilized. The yielded and unyielded regions around the sphere are shown in the Fig. 1.

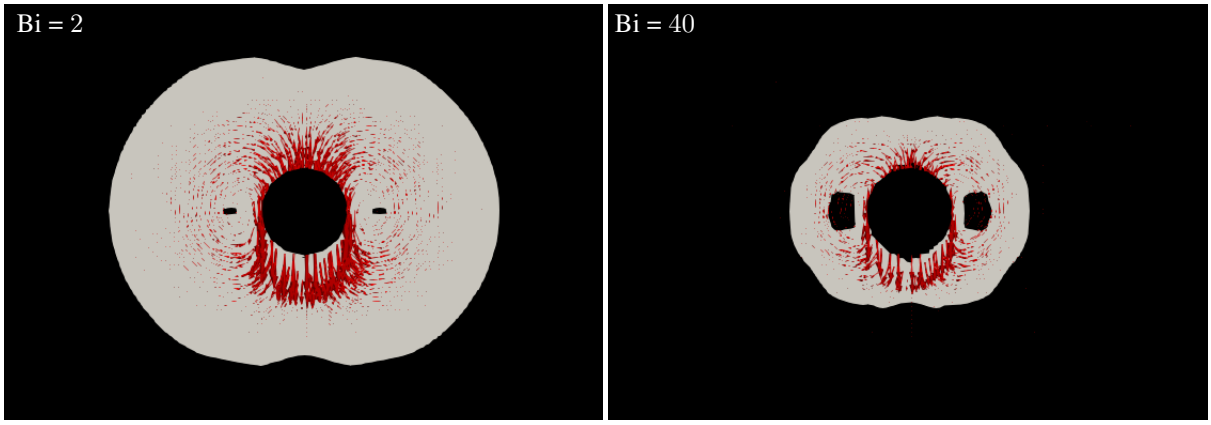

Figure 1. Velocity vectors (red) and unyielded (black) / yielded (gray) regions for flow around a fixed sphere with Reynolds number equal to 1.

The yield surface was delimited by $\tau = 10^4$ to reduce the numerical noise, it acquired the truncated toroid form expected in this flow[23]. The fluid displacement in the fore section of the sphere creates a circulation pattern

that causes the formation of an unyielded region inside the yielded fluid [24]. The indentation in the fore and aft sections of the yield surface, due to the reduced stress, are also present. These results demonstrate that the numerical model is capable to account for a correct representation of the Bingham fluid flow.

4 Results

To understand the events which will occur during the particle settling in a thixotropic fluid the following simulation parameters are utilized. A particle with diameter D is positioned $25.2D$ from the bottom of a rectangular domain with dimensions $6.7D \times 6.7D \times 26.7D$ which contain an initially unstructured thixo-viscoplastic fluid. This fluid has a dynamic yield stress equal to zero, $\tau_y^D = 0$, while its static yield stress is modified to change the yield number $Y_G = 3\tau_y^S/gD\,(\rho_p - \rho_f)$. The plastic viscosity is kept constant at $\eta_p/\sqrt{gD^3} = 6.7 \times 10^{-3}$. The breakdown parameter is $k_1/\sqrt{D/g} = 6.65 \times 10^{-3}$ and the build-up parameter is $k_2 = 1 \times 10^{-4}$. In this study two equilibrium time values $t_{eq}/\sqrt{D/g} = 1.6 \times 10^{-6}$ and 4.8×10^{-6}, with $\tau_g = 0.5001$, are evaluated. The rectangular domain is discretized with $150 \times 150 \times 600$ lattices, while the spherical particle is composed of 1158 Lagrangian nodes, with a density ratio of $\rho_p/\rho_f = 1.16$. The modified yield number was varied from 0 to 0.156 and the results for trajectory and velocity are presented in Fig. 2.

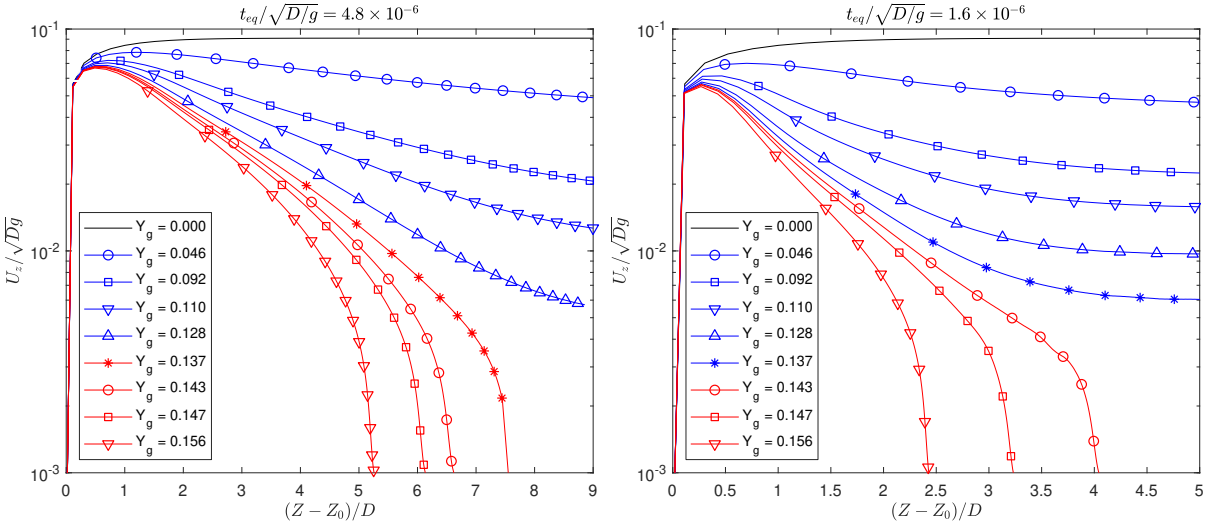

Figure 2. Trajectory and velocity of a spherical particle with different Y_G settling in a thixo-viscoplastic fluid with $t_{eq}/\sqrt{D/g} = 1.6 \times 10^{-6}$ and 4.8×10^{-6}. Red: Particle stopped / Blue: finite terminal velocity.

Analyzing the results for the highest equilibrium time, the particle reaches a terminal velocity when $Y_G \leq 0.128$ while for $Y_G \geq 0.137$ it does not have enough weight to break the fluid and it is consequently retained. This indicates that the critical yield number is between 0.137 and 0.143 for this equilibrium time. If the equilibrium time decreases, the thixotropic fluid takes a shorter time to reach equilibrium, and this causes the particle to maintain the high initial velocity for a reduced period Fig. 2.b. Reducing the equilibrium time also decreases the maximum and terminal velocities achieved, as a consequence of higher average yield stress in the flow. It was observed a 12% drop in the terminal velocity when $Y_G = 0.046$, the velocity drop kept increasing exponentially with Y_G until the particle is completely still. As consequence, the critical yield numbed move to be between 0.137 and 0.143, which are close of the result of 0.143 obtained by Beris et al. [23] and 0.145 by Tabuteau et al. [3] in a Bingham fluid. Essentially, the Bingham model could be modeled as thixo-viscoplastic fluid with instantaneous build-up rate, in other words with, a equilibrium time equal to zero.

Another important aspect is to understand the evolution of the yield surface and the structural parameter field over time, which for the values of $Y_G = 0.148$ and 0.137 are represented in Fig. 3. At very short times there is no apparent difference in the fluid structure, when the structuring level of the undisturbed fluid $\lambda_\infty = 0.64$. The yielded surface is similar to the one formed when settling a Bingham fluid, with a sightly asymmetry between the fore and aft sections. This changes when the fluid reaches the maximum structuring level, $\lambda_\infty = 1$. On this point, as expected the structural parameter decreases near the particle wall and in the frontier between the yielded and unyielded regions, which leaves a trail of reduced yield stress in the path that the particle traveled. But the opposite

also happens, the unyielded regions inside the yielded do not totally breakdown, which causes the appearance of a connection with the outside unyielded fluid when $Y_G = 0.143$. When $Y_G = 0.137$ this will simply increase the size of the unyielded region, but not create the connection. A new unyielded region will appear in the aft section, this is associated with the stagnation point which occurs behind a sphere. As the time progresses further, for $Y_G = 0.143$ the particle is now is still with the fluid totally yielded but with some regions where $\lambda < 1$ which are still recovering from the shear caused by the particle. Meanwhile for $Y_G = 0.137$ the particle continues to settle in a steady-state.

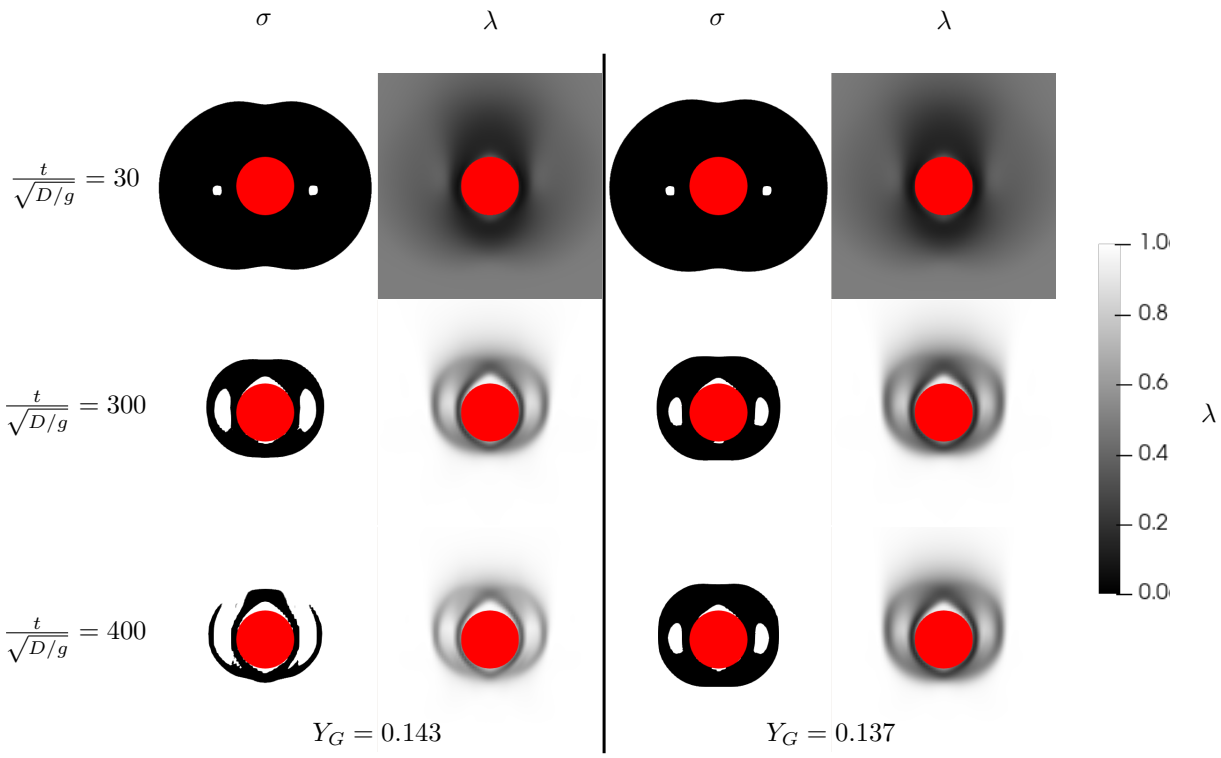

Figure 3. Time evolution for the yield surface and structural parameter when $Y_G = 0.143$ and 0.137, with $t_{eq}/\sqrt{D/g} = 1.6 \times 10^{-6}$ and $\tau_g = 0.5001$.

5 Conclusions

In this study, it was investigated the settling phenomenon of a spherical particle in a thixo-viscoplastic fluid. The results were obtained through the use of the lattice Boltzmann method coupled with the immersed boundary method. Thixotropy was modeled using a modified micro-structural indirect model. A selection of parameters allowed the reduction to a Bingham model, which was used to validate the numerical method. At initial times, the particle accelerates similar to a Newtonian fluid, due to the reduced value of the yield stress. As the fluid builds-up to a structured state the particle velocity reduces, until it reaches a steady-state. The steady-state can be divided into two states: finite terminal velocity or stopped. The separation of these states is characterized by the critical yield number. It was noted that yield number value changes depending on time-dependent parameters of the model, where a longer equilibrium time reduced the yield stress necessary to stop the particle. When the fluid is totally structured, the strain caused by the settling particle causes a reduced breakdown rate, which consequently leads to higher yield stress near the particle. This effect also increases the size of unyielded regions near the particle, to the point where it will connect with the outside unyielded regions. Overall the method was capable to model the thixo-viscoplastic behavior, as well as reduce the particle velocity until stop. Furthermore, the method can be expanded to accommodate different thixo-viscoplastic models, and model higher numbers of particles along with different shapes.

Acknowledgements. This study was financed in part by the Coordenação de Aperfeiçoamento de Pessoal de Nível

Superior - Brasil (CAPES) - Finance Code 001

Authorship statement. The authors hereby confirm that they are the sole liable persons responsible for the authorship of this work, and that all material that has been herein included as part of the present paper is either the property (and authorship) of the authors, or has the permission of the owners to be included here.

References

[1] Mewis, J. & Wagner, N. J., 2009. Thixotropy. *Advances in Colloid and Interface Science*, vol. 147-148, n. C, pp. 214–227.
[2] Bird, R. B., Armstrong, R. C., & Hassager, O., 1987. *Dynamics of Polymerics Liquids*. Wiley, 2 edition.
[3] Tabuteau, H., Coussot, P., & de Bruyn, J. R., 2007. Drag force on a sphere in steady motion through a yield-stress fluid. *Journal of Rheology*, vol. 51, n. 1, pp. 125–137.
[4] Ferroir, T., Huynh, H. T., Chateau, X., & Coussot, P., 2004. Motion of a solid object through a pasty (thixotropic) fluid. *Physics of Fluids*, vol. 16, n. 3, pp. 594–601.
[5] Moseley, K., Fairweather, M., & Harbottle, D., 2019. Settling dynamics of two identical vertically aligned spheres in a thixotropic fluid. *Journal of Non-Newtonian Fluid Mechanics*, vol. 271, n. June, pp. 104146.
[6] Barnes, H. A., 1997. Thixotropy—a review. *Journal of Non-Newtonian Fluid Mechanics*, vol. 70, n. 1-2, pp. 1–33.
[7] Bhatnagar, P. L., Gross, E. P., & Krook, M., 1954. A Model for Collision Processes in Gases. I. Small Amplitude Processes in Charged and Neutral One-Component Systems. *Physical Review*, vol. 94, n. 3, pp. 511–525.
[8] Latt, J. & Chopard, B., 2006. Lattice Boltzmann method with regularized pre-collision distribution functions. *Mathematics and Computers in Simulation*, vol. 72, n. 2-6, pp. 165–168.
[9] Philippi, P. C., Hegele, L. A., dos Santos, L. O. E., & Surmas, R., 2006. From the continuous to the lattice Boltzmann equation: The discretization problem and thermal models. *Physical Review E*, vol. 73, n. 5, pp. 056702.
[10] Guo, Z., Zheng, C., & Shi, B., 2002. Discrete lattice effects on the forcing term in the lattice Boltzmann method. *Physical Review E*, vol. 65, n. 4, pp. 046308.
[11] Silva, G. & Semiao, V., 2012. First-and second-order forcing expansions in a lattice Boltzmann method reproducing isothermal hydrodynamics in artificial compressibility form. *Journal of Fluid Mechanics*, vol. 698, pp. 282–303.
[12] Lugarini, A., Franco, A. T., & Philippi, P. C., 2020. Lattice Boltzmann method for viscoplastic fluid flow based on regularzation of ghost moments.
[13] Houska, M., 1980. *Inzenyrske aspekty reologie tixotropnich kapalin*. PhD thesis, Technical University of Prague.
[14] Chopard, B., Falcone, J. L., & Latt, J., 2009. The lattice Boltzmann advection-diffusion model revisited. *European Physical Journal: Special Topics*, vol. 171, n. 1, pp. 245–249.
[15] Ginzburg, I., D'Humières, D., & Kuzmin, A., 2010. Optimal stability of advection-diffusion lattice boltzmann models with two relaxation times for positive/negative equilibrium. *Journal of Statistical Physics*, vol. 139, n. 6, pp. 1090–1143.
[16] Peskin, C. S., 1972. Flow patterns around heart valves: A numerical method. *Journal of Computational Physics*, vol. 10, n. 2, pp. 252–271.
[17] Feng, Z.-G. & Michaelides, E. E., 2004. The immersed boundary-lattice Boltzmann method for solving fluid–particles interaction problems. *Journal of Computational Physics*, vol. 195, n. 2, pp. 602–628.
[18] Dash, S. M., Lee, T. S., Lim, T. T., & Huang, H., 2014. A flexible forcing three dimension IB-LBM scheme for flow past stationary and moving spheres. *Computers and Fluids*, vol. 95, pp. 159–170.
[19] Feng, Z.-G. & Michaelides, E. E., 2009. Robust treatment of no-slip boundary condition and velocity updating for the lattice-Boltzmann simulation of particulate flows. *Computers & Fluids*, vol. 38, n. 2, pp. 370–381.
[20] Ladd, A. J. C. & Verberg, R., 2001. Lattice-Boltzmann Simulations of Particle-Fluid Suspensions. *Journal of Statistical Physics*, vol. 104, n. September, pp. 1191–1251.
[21] Krüger, T., Kusumaatmaja, H., Kuzmin, A., Shardt, O., Silva, G., & Viggen, E. M., 2017. *The Lattice Boltzmann Method*, volume 23 of *Graduate Texts in Physics*. Springer International Publishing, Cham, 1 edition.
[22] Blackery, J. & Mitsoulis, E., 1997. Creeping motion of a sphere in tubes filled with a Bingham plastic material. *Journal of Non-Newtonian Fluid Mechanics*, vol. 70, n. 1-2, pp. 59–77.
[23] Beris, A. N., Tsamopoulos, J. A., Armstrong, R. C., & Brown, R. A., 1985. Creeping motion of a sphere through a Bingham plastic. *Journal of Fluid Mechanics*, vol. 158, n. July 2014, pp. 219–244.
[24] Ansley, R. W. & Smith, T. N., 1967. Motion of spherical particles in a Bingham plastic. *AIChE Journal*, vol. 13, n. 6, pp. 1193–1196.